

Experimental Evidence for Transverse Wobbling in ^{105}Pd

J. Timár,^{1,*} Q. B. Chen,² B. Kruzcicz,¹ D. Sohler,¹ I. Kuti,¹ S. Q. Zhang,³ J. Meng,³ P. Joshi,⁴ R. Wadsworth,⁴ K. Starosta,⁵ A. Algora,^{1,6} P. Bednarczyk,⁷ D. Curien,⁸ Zs. Dombrádi,¹ G. Duchêne,⁸ A. Gizon,⁹ J. Gizon,⁹ D. G. Jenkins,⁴ T. Koike,¹⁰ A. Krasznahorkay,¹ J. Molnár,¹ B. M. Nyakó,¹ E. S. Paul,¹¹ G. Rainovski,¹² J. N. Scheurer,¹³ A. J. Simons,⁴ C. Vaman,¹⁴ and L. Zolnai¹

¹*Institute for Nuclear Research, Hungarian Academy of Sciences, Pf. 51, 4001 Debrecen, Hungary*

²*Physik-Department, Technische Universität München, D-85747 Garching, Germany*

³*State Key Laboratory of Physics and Technology,*

School of Physics, Peking University, Beijing 100871, China

⁴*Department of Physics, University of York, York, YO10 5DD, United Kingdom*

⁵*Department of Chemistry, Simon Fraser University, Burnaby, British Columbia V5A 1S6, Canada*

⁶*Instituto de Física Corpuscular, CSIC-University of Valencia, E-46071, Valencia, Spain*

⁷*Institute of Nuclear Physics Polish Academy of Sciences, PL-31342 Krakow, Poland*

⁸*Université de Strasbourg, CNRS, IPHC UMR7178, 67037 Strasbourg, France*

⁹*LPSC, IN2P3-CNRS/UJF, F-38026 Grenoble-Cedex, France*

¹⁰*Graduate School of Science, Tohoku University, Sendai, 980-8578, Japan*

¹¹*Oliver Lodge Laboratory, Department of Physics,*

University of Liverpool, Liverpool L69 7ZE, United Kingdom

¹²*Faculty of Physics, St. Kliment Ohridski University of Sofia, 1164 Sofia, Bulgaria*

¹³*Université Bordeaux 1, IN2P3- CENBG - Le Haut-Vigneau BP120 33175, Gradignan Cedex, France*

¹⁴*Department of Physics and Astronomy, SUNY, Stony Brook, New York, 11794-3800, USA*

(Dated: January 18, 2019)

New rotational bands built on the $\nu(h_{11/2})$ configuration have been identified in ^{105}Pd . Two bands built on this configuration show the characteristics of transverse wobbling: the $\Delta I=1$ transitions between them have a predominant E2 component and the wobbling energy decreases with increasing spin. The properties of the observed wobbling bands are in good agreement with theoretical results obtained using constrained triaxial covariant density functional theory and quantum particle rotor model calculations. This provides the first experimental evidence for transverse wobbling bands based on a one-neutron configuration, and also represents the first observation of wobbling motion in the $A\sim 100$ mass region.

PACS numbers: 21.10.Hw, 21.10.Re, 21.60.Ev, 23.20.Lv, 27.60.+j

Nuclear wobbling motion was initially discussed by Bohr and Mottelson [1]. This type of rotation is predicted to occur in triaxially deformed nuclei. The nucleus rotates around the principal axis having the largest moment of inertia and this axis executes harmonic oscillations about the space-fixed angular momentum vector. Its analog in classical mechanics is the motion of a free asymmetric top, while in quantal systems a corresponding example would be the rotation of molecules having different moments of inertia for the three principal axes. In nuclei, the expected energy spectra related to this motion are characterized by a series of rotational E2 bands corresponding to the different oscillation quanta (n). The signature quantum number of two consecutive bands is different, thus the yrast and yrare bands (corresponding to $n=0$ and $n=1$, respectively), look like signature partner bands with large signature splitting. The yrare band decays by $\Delta I=1$ M1+E2 transitions to the yrast band. However, contrary to the case of signature partners, the multipole mixing ratios are very large, and the transitions have predominantly E2 character. Furthermore, the energy separation between the yrare and yrast

bands, the wobbling energy, is expected to increase with increasing spin. Although Bohr and Mottelson predicted this motion for even-even nuclei where no intrinsic angular momentum is involved, the phenomenon in this simple form has not been experimentally documented to date.

The first experimental evidence for nuclear wobbling motion was reported in the odd-proton ^{163}Lu ($Z=71$) nucleus [2, 3] and later in the ^{161}Lu , ^{165}Lu , ^{167}Lu nuclei [4–6], as well as in ^{167}Ta ($Z=73$) [7]. In these nuclei the wobbling mode is observed in the triaxial strongly deformed bands corresponding to the $\pi(i_{13/2})$ intruder configuration. Recently, wobbling motion was reported in ^{135}Pr ($Z=59$), where the wobbling bands have normal deformation and they are built on the $\pi(h_{11/2})$ configuration [8]. The expected different signature values and the predominant E2 character of the $\Delta I=1$ transitions between the bands have been observed for all the above cases. However, the wobbling energy has been found to decrease with increasing spin contrary to theoretical expectations. Frauendorf and Dönau [9] interpreted this behavior as the consequence of the perpendicular orientation of the odd particle's angular momentum to the rotational axis, and they suggested to name the phenomenon as “transverse wobbling”. This interpretation differs from that previously published for the Lu and Ta isotopes, and gener-

* Corresponding author: timar@atomki.hu

ated great theoretical interest to clarify the situation using different models [10–19]. Very recently another type of the wobbling motion has been claimed in ^{133}La , the “longitudinal wobbling”, where the wobbling energy was found to increase with increasing spin [20]. It is worth noting that all the wobbling bands observed so far correspond to a configuration of one proton coupled to the core. In this Letter, we report on experimental evidence for transverse wobbling motion in ^{105}Pd ($Z=46$, $N=59$). This is the first observation of transverse wobbling motion based on a one-neutron configuration, and also the first observation of wobbling motion in the $A\sim 100$ mass region.

High-spin states in ^{105}Pd were populated using the $^{96}\text{Zr}(^{13}\text{C},4n)$ reaction. The ^{13}C beam was provided by the Vivitron accelerator at IReS, Strasbourg. The beam impinged upon a stack of two self supporting metallic foil targets being enriched to 86% in ^{96}Zr , and each having a thickness of ~ 0.6 mg/cm 2 . The emitted γ -rays were detected by the EUROBALL IV [21] spectrometer equipped with 15 Cluster detectors at backward angles and 24 Clover detectors at 90° relative to the beam direction. Contaminants from the charged-particle reaction channels were eliminated using the highly efficient DIAMANT charged-particle detector array consisting of 88 CsI detectors [22, 23] as an off-line veto. A total of $\sim 2 \times 10^9$ triple- and higher-fold coincidence events were obtained and stored onto magnetic tapes.

The level scheme of ^{105}Pd was constructed using the Radware analysis package [24] on the basis of the triple-coincidence relations, as well as energy and intensity balances of the observed γ rays. Several new rotational bands have been observed in ^{105}Pd . Among them there are negative-parity quadrupole bands with probable neutron $h_{11/2}$ configuration. Two of these bands have opposite signature than the previously known, yrast neutron $h_{11/2}$ band. Fig. 1 shows the yrast neutron $h_{11/2}$ band (band A) up to spin $43/2 \hbar$ and the two newly identified bands (bands B and C).

Linear polarizations and directional correlation from oriented states (DCO) ratios [25–28] were derived for the transitions of sufficient intensity. The observed values for the transitions relevant to the focus of the present Letter are compared in Fig. 2 with the values of different multiplicities and mixing ratios calculated for the experimental geometry. For the DCO ratio analysis we used stretched E2 gating transitions, the attenuation coefficients of incomplete alignment were fitted to the known strong 1100 keV E2 and 1331 keV E1 transitions [29] in ^{105}Pd assuming pure stretched E2 and E1 multiplicities for them, respectively. Our analysis resulted a mixing ratio of $-0.37(8)$ for the 442 keV lowest inband M1+E2 transition in ^{105}Pd which reproduced well the $-0.33(13)$ value reported in Ref. [29]. The 1331 keV and 442 keV transitions are not shown in Fig. 1. Details of the experimental setup and data analysis, as well as the full level scheme, will be provided in a forthcoming publication [30].

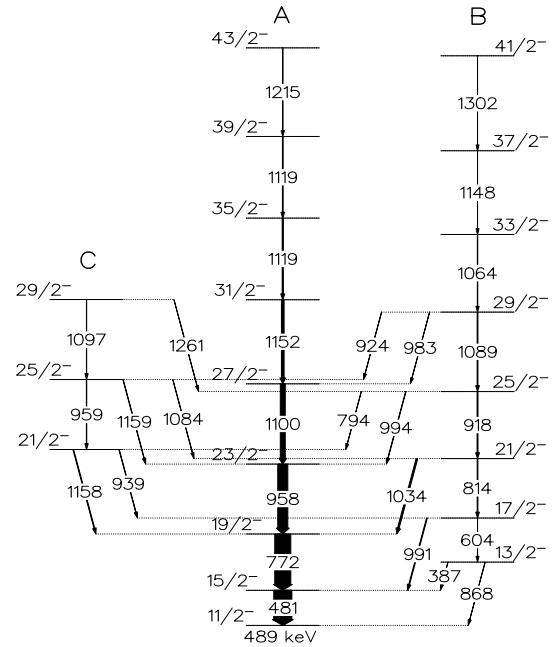


FIG. 1. Partial level scheme of ^{105}Pd observed in the present work and relevant to the focus of the present Letter. Widths of the lines are proportional with the transition intensities.

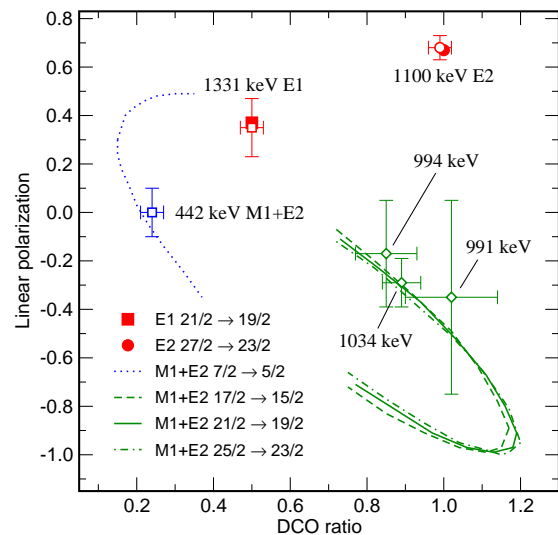


FIG. 2. Experimental (symbols with X and Y error bars) and calculated (full square, circle, as well as full, dashed, dot-dashed and dotted lines) DCO and linear polarization values for the linking transitions between bands A and B, and for three known-multipolarity transitions. In the full, dashed and dot-dashed lines the δ multipole mixing ratio value varies from 0.24 (lower end) to 3.2 (upper end). In the dotted line δ varies from -0.12 (lower end) to -7.1 (upper end).

Band A has been reported in Refs. [29, 31] with spin-parity values firmly assigned to the states up to spin $31/2 \hbar$. Data from the present experiment confirm the previously reported values. The $17/2^-$, $21/2^-$ and $25/2^-$ states of band B and the $21/2^-$ state of band C were reported in Ref. [29] as non-band levels. However, the levels belonging to bands B and C have been identified as rotational bands first in the present experiment. The DCO and linear polarization values derived for the 814 keV, 918 keV, 1089 keV and 1064 keV transitions agree well with stretched E2 multipolarity, confirming the E2-band character of band B. As it is seen in Fig. 2, the measured DCO and linear polarization values for the 991 keV, 1034 keV and 994 keV transitions are in good agreement with $\Delta I=1$ M1+E2 multipolarity at large, $\delta=1.8(5)$, $2.3(3)$, $2.7(6)$ multipole mixing ratios, respectively. Thus, these transitions have predominantly E2 characters, however, they cannot be pure $\Delta I=2$ E2 transitions because for such transitions the linear polarization values are expected to be between 0.65 and 0.7, like in the case of the 1100 keV gamma transition, contrarily to the measured negative values. Therefore, the observed DCO and polarization values allow only the $17/2^-$, $21/2^-$ and $25/2^-$ spin-parity values for the initial states of the 991 keV, 1034 keV and 994 keV transitions, respectively. Strictly speaking, spins less by one or two units would also be allowed by the DCO and polarization data. However, it is very rare that levels of rotational bands decay to the same-spin or higher-spin states of another band, and in those cases they also decay to lower-spin levels of the other band. Existence of such transitions to lower spin states was excluded by the observed data in the present case.

The lowest-energy state of band C is fed by the 794 keV transition from the $25/2^-$ state of band B and decays by the 939 keV transition to the $17/2^-$ state of band B. As the M2, M3 and E3 transitions are not competitive with E2 and M1 transitions, the 794 keV and the 939 keV transitions can only be stretched E2 transitions. Thus the spin-parity of the lowest-energy state of band C can only be $21/2^-$. Similarly, the second state of band C is linked to the $21/2^-$ and to the $29/2^-$ states of band B. Thus, its spin-parity can only be $25/2^-$. This also confirms the E2-band character of band C. The adopted spin-parity assignments for the four previously known levels of bands B and C are consistent with those reported in Ref. [29].

Band C decays to band A by the 1158 keV and 1159 keV transitions. Linear polarization value of $-0.6(3)$ was derived for the sum of the two transitions. Unfortunately, no linear polarization values could be deduced separately for the two transitions because of their close energies. DCO value could not be derived even for the sum of the two transitions because their energies are close to that of the strong 1152 keV transition in band A. The fact that the 1158 keV, 1159 keV and 1152 keV transitions are all in coincidence with the intense gamma rays which could be used as coincidence gates, caused further difficulties

in the analysis. The deduced linear polarization value agrees well with the multipolarity expected for the 1158 keV and 1159 keV transitions from the above spin-parity assignments for the band C states: namely that they are $\Delta I=1$ M1+E2 transitions. However, it allows both small ($0 \leq \delta \leq 0.5$) and large ($1 \leq \delta \leq 2.4$) mixing ratios.

The observed three bands show the features of a pair of wobbling bands with oscillation quanta zero and one (bands A and B, respectively) and the signature partner band of band A (band C). Indeed, the multiplicities of the lowest-lying linking transitions between bands B and A are M1+E2 with large, $\delta=1.8(5)$, $2.3(3)$, $2.7(6)$ multipole mixing ratios for the 991 keV, 1034 keV and 994 keV transitions, respectively. These mixing ratios mean around 80% (calculated as $\delta^2/(1 + \delta^2)$) E2 content, which is expected for the wobbling band, but not expected for the signature partner. We note that the 991 keV, 1034 keV and 994 keV transitions were also reported in Ref. [29] and $\delta=0.46(10)$ as well as $\delta=0.62(18)$ were derived for the 991 keV and 1034 keV transitions, respectively, from angular distribution measurement. While the present DCO results also allow $\delta=0.59(20)$ and $0.40(6)$ values for the two transitions, respectively, the linear polarization data disagree with these smaller mixing ratios, but strongly support the larger $\delta=1.8(5)$ and $2.3(3)$ values.

Band C is a candidate for the signature partner of band A. The two bands have the same parity and similar alignments [30] but opposite signature. Furthermore, band C decays to band A by the 1158 keV and 1159 keV transitions. Although the mixing ratios of these transitions could not be derived unambiguously, the possible smaller mixing ratio value deduced from the present experiment is in a good agreement with this scenario. In Ref. [29] a mixing ratio of $\delta=1.3(9)$ was reported for the 1158 keV transition. Due to the large uncertainty this value can allow a rather small mixing ratio, thus it can be in agreement with the signature partner interpretation, too.

The difference between the mixing ratio values measured for the linking M1+E2 transitions between the wobbling bands in ^{135}Pr and in ^{105}Pd is their opposite signs. While the sign is positive in ^{105}Pd , it is negative in ^{135}Pr . The sign of the mixing ratio value is determined by the sign of the M1 matrix element assuming that the quadrupole deformation is of same type. The sign of the M1 matrix element is proportional with the $(g_p - g_R)$ factor [1], where g_R is the rotational gyromagnetic factor. Its value is approximately Z/A , which is ~ 0.4 for both nuclei. However, g_p , the gyromagnetic factor of the odd particle, is different for the protons and the neutrons moving in high- j intruder ($j = l + 1/2$) orbitals. It has a large positive value (>1) for protons, while it has a negative sign for neutrons. Thus, the sign of the $(g_p - g_R)$ factor is opposite for high- j protons and neutrons [32].

In order to explore the nature of the observed rotational band structures in ^{105}Pd , they have been studied by the constrained triaxial covariant density functional

theory (CDFT) [33, 34] as well as the quantum particle rotor model (PRM) [9, 19, 35–38]. The configuration-fixed CDFT calculations [33, 34] with the effective interaction PC-PK1 [39] reveal that the $\nu(1h_{11/2})^1$ configuration has a triaxial shape of $\beta = 0.27$ and $\gamma = 25^\circ$, which fulfills the conditions required for the presence of wobbling bands.

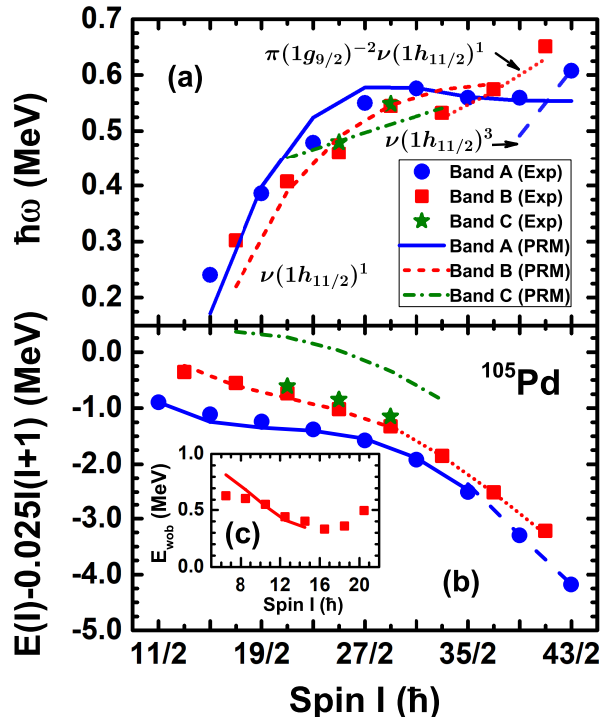


FIG. 3. Experimental and PRM rotational frequency (a) as well as energies minus a rotor contribution (b) as functions of spin I for the bands A, B, and C in ^{105}Pd . Inset (c): Wobbling energies associated with the wobblers-band pair A and B.

With the configuration and deformation parameters obtained, it is straightforward to perform PRM [9, 19, 37, 38] calculations in order to study the energy spectra and electromagnetic transition probabilities for the observed rotational sequences in ^{105}Pd . In the PRM calculations, the neutron particle is described by a single- j shell Hamiltonian [40] and the pairing effect is included using the standard BCS quasiparticle approximation with the empirical pairing gap $\Delta = 12/\sqrt{A} = 1.17$ MeV and the Fermi surface located at the beginning of the $h_{11/2}$ subshell. The triaxial rotor is parametrized by three angular-momentum-dependent moments of inertia $\mathcal{J}_i = a_i\sqrt{1 + bI(I+1)}$ [41, 42] (known as the ab formula) to take into account the soft character of the potential energy surface revealed by CDFT calculations [43]. Here, $i = m, s, l$ denotes the medium, short, and long axes, respectively, and the corresponding parameters $a_{m,s,l} = 5.89, 3.74, 1.27 \hbar^2/\text{MeV}$ and $b = 0.023 \hbar^{-2}$ are determined by fitting to the energy spectra of bands A and B.

The calculated rotational frequency ($\hbar\omega(I) = [E(I) - E(I-2)]/2$) and energy spectra as functions of spin I for bands A (solid line), B (short dash line), and C (short dash-dot line), in comparison with those of the experimental data, are shown in Fig. 3. It is seen that the PRM calculations can reproduce bands A and B well. For band C, the energies are overestimated by about 500 keV. A similar problem is also seen in Ref. [8] for ^{135}Pr .

For band A, the rotational frequency is almost constant from spin $I = 27/2$ to $39/2$, which presents an upbend phenomenon and is understood by the gradual alignment of a $h_{11/2}$ neutron pair. Such an alignment process can be reproduced by the PRM calculations due to the use of angular-momentum-dependent moments of inertia. After the upbending, the configuration becomes a three-quasiparticle configuration $\nu(1h_{11/2})^3$, whose quadrupole deformation parameters are $\beta = 0.29$ and $\gamma = 10^\circ$ from the CDFT calculations, and the data can be reproduced by the PRM (dash line) with the moments of inertia taken as irrotational flow type $\mathcal{J}_k = \mathcal{J}_0 \sin^2(\gamma - 2k\pi/3)$ with $\mathcal{J}_0 = 20 \hbar^2/\text{MeV}$.

For band B, the experimental rotational frequency has a discontinuity between $I = 29/2$ and $33/2$, which is understood by the alignment of a proton $g_{9/2}$ pair given that its alignment is $2\hbar$ smaller than that of band A in the region $I \geq 39/2$. Hence, the unpaired valence nucleon configuration for band B at $I \geq 33/2$ is assigned as $\pi(1g_{9/2})^{-2} \otimes \nu(1h_{11/2})^1$, whose deformation parameters are $\beta = 0.25$ and $\gamma = 28^\circ$ according to the CDFT calculations. With this configuration and $\mathcal{J}_0 = 21 \hbar^2/\text{MeV}$, the corresponding experimental rotational frequencies and energies can be well reproduced as shown in Fig. 3 (short dotted line), and thus supports the configuration assignment.

With the successful reproduction of the energy spectra of bands A and B, the wobbling energy E_{wob} (as defined in Ref. [8]) can also be reproduced by the PRM calculations, as shown in Fig. 3(c). In agreement with the experimental observation, the calculated wobbling energy decreases with spin until $I = 29/2$, which presents the characteristic of a transverse wobblers. Note that the increasing energy difference between bands A and B in the region $I \geq 33/2$ cannot be interpreted as evidence of a longitudinal wobblers [9], since their configurations are different as discussed above.

In Table I, the experimental and theoretical mixing ratios δ as well as the transition probability ratios $B(M1)_{\text{out}}/B(E2)_{\text{in}}$ and $B(E2)_{\text{out}}/B(E2)_{\text{in}}$ for the transitions from band B to A in ^{105}Pd are listed. It is known that $B(E2)_{\text{out}}/B(E2)_{\text{in}}$ is proportional to $\tan^2 \gamma$ [1, 13]. It is found that the PRM results are in good agreement with the data. Thus, the microscopic input of the triaxial deformation parameter from the CDFT calculation is appropriate.

The mixing ratios δ and $B(M1)_{\text{out}}/B(E2)_{\text{in}}$ are proportional to Q_0/g_{eff} and $(g_{\text{eff}}/Q_0)^2$, respectively, with Q_0 the intrinsic quadrupole moment and $g_{\text{eff}} = g_{\nu h_{11/2}} - g_R$ the effective gyromagnetic factor. It was found that in

TABLE I. The experimental and theoretical multipole mixing ratios δ as well as the transition probability ratios $B(M1)_{\text{out}}/B(E2)_{\text{in}}$ and $B(E2)_{\text{out}}/B(E2)_{\text{in}}$ for the transitions from band B to A in ^{105}Pd .

$I_i^\pi \rightarrow I_f^\pi$	E_γ (keV)	δ		$\frac{B(M1)_{\text{out}}}{B(E2)_{\text{in}}} \left(\frac{\mu_N^2}{e^2 b^2} \right)$		$\frac{B(E2)_{\text{out}}}{B(E2)_{\text{in}}}$	
		Exp	PRM	Exp	PRM	Exp	PRM
$17/2^- \rightarrow 15/2^-$	991	1.8 ± 0.5	2.38	0.162 ± 0.097	0.105	0.66 ± 0.18	0.736
$21/2^- \rightarrow 19/2^-$	1034	2.3 ± 0.3	2.30 ^a	0.089 ± 0.026	0.069	0.60 ± 0.09	0.465
$25/2^- \rightarrow 23/2^-$	994	2.7 ± 0.6	1.99	0.029 ± 0.016	0.057	0.34 ± 0.07	0.329

^a Normalization point, see text.

the PRM calculations, the $B(M1)_{\text{out}}$ values would be overestimated by about a factor of 3–10 [8, 9]. This is due to the scissors mode which is mixed with the wobbling motion and cannot be considered in the PRM calculations [44]. Bearing this in mind, a quenching factor of 0.36 for g_{eff} is introduced in the calculation in order to reproduce the value of δ for the transition $21/2^- \rightarrow 19/2^-$. With this treatment, the other experimental δ values as well as the $B(M1)_{\text{out}}/B(E2)_{\text{in}}$ values can also be reproduced. The large $B(E2)_{\text{out}}/B(E2)_{\text{in}}$ and small $B(M1)_{\text{out}}/B(E2)_{\text{in}}$ values further support the wobbling interpretation for the bands A and B in the region $I \leq 29/2$.

With the successful reproduction of the energy spectra and electromagnetic transitions in ^{105}Pd , the angular momentum geometries of bands A and B are examined in the PRM [19]. Indeed, it is found that the neutron angular momenta in bands A and B are similar and mainly align along the s -axis in the region $I \leq 25/2$. The wave functions of band A are symmetric and peaked at the s -axis below $I = 23/2$, which indicates a principal axis rotation around the s -axis. At $I = 29/2$, the rotational mode of band A changes to a planar rotation. With one-phonon excitation, the wave functions of band B are antisymmetric and have a node around the s -axis. These features are the same as in the case of ^{135}Pr [19], thus further confirming the transverse wobbling interpretation for bands A and B of ^{105}Pd in the region $I \leq 29/2$.

In summary, we have studied nuclear transverse wobbling in ^{105}Pd , where the wobbling bands are based on the $\nu(h_{11/2})$ one-neutron configuration. The predomi-

nant E2 character of the $\Delta I=1$ M1+E2 transitions between the wobbling bands is confirmed by the precise measurement of DCO values and linear polarization data. The transverse wobbling nature of these bands conforms well to results from calculations using constrained triaxial covariant density functional theory and the quantum particle rotor model. This observation provides the first experimental evidence for transverse wobbling bands based on a one-neutron configuration, and is also the first observation of wobbling motion in the $A \sim 100$ mass region.

The authors thank Professor C. M. Petrache for stimulating and useful discussions. This work was supported by the National Research, Development and Innovation Fund of Hungary, financed under the K18 funding scheme with project nos. K128947 and K124810. This work was also supported by the European Regional Development Fund (Contract No. GINOP-2.3.3-15-2016-00034), as well as by Deutsche Forschungsgemeinschaft (DFG) and National Natural Science Foundation of China (NSFC) through funds provided to the Sino-German CRC 110 ‘‘Symmetries and the Emergence of Structure in QCD’’, the National Key R&D Program of China (Contract No. 2018YFA0404400), the NSFC under Grants No. 11335002 and No. 11621131001, the UK STFC under grant no. ST/P003885/1, and the Spanish Ministerio de Economía y Competitividad under Grant No. FPA2014-52823-C2-1-P and the program Severo Ochoa (SEV-2014-0398). I.K. was supported by National Research, Development and Innovation Office NKFIH, contract number PD 124717.

-
- | | |
|---|--|
| <p>[1] A. Bohr and B. R. Mottelson, <i>Nuclear Structure, Vol. II</i> (Benjamin, New York, 1975).</p> <p>[2] S. W. Ødegard, G. B. Hagemann, D. R. Jensen, M. Bergström, B. Herskind, G. Sletten, S. Törmänen, J. N. Wilson, P. O. Tjøm, I. Hamamoto <i>et al.</i>, Phys. Rev. Lett. 86, 5866 (2001).</p> <p>[3] D. R. Jensen, G. B. Hagemann, I. Hamamoto, S. W. Ødegard, B. Herskind, G. Sletten, J. N. Wilson, K. Spohr, H. Hübel, P. Bringel <i>et al.</i>, Phys. Rev. Lett. 89, 142503 (2002).</p> <p>[4] P. Bringel, G. Hagemann, H. Hübel, A. Al-khatib, P. Bednarczyk, A. Bürger, D. Curien, G. Gangopadhyay, B. Herskind, D. Jensen <i>et al.</i>, Eur. Phys. J. A 24, 167</p> | <p>(2005).</p> <p>[5] G. Schönwaßer, H. Hübel, G. B. Hagemann, P. Bednarczyk, G. Benzoni, A. Bracco, P. Bringel, R. Chapman, D. Curien, J. Domscheit <i>et al.</i>, Phys. Lett. B 552, 9 (2003).</p> <p>[6] H. Amro, W. C. Ma, G. B. Hagemann, R. M. Diamond, J. Domscheit, P. Fallon, A. Gørgen, B. Herskind, H. Hübel, D. R. Jensen <i>et al.</i>, Phys. Lett. B 553, 197 (2003).</p> <p>[7] D. J. Hartley, R. V. F. Janssens, L. L. Riedinger, M. A. Riley, A. Aguilar, M. P. Carpenter, C. J. Chiara, P. Chowdhury, I. G. Darby, U. Garg <i>et al.</i>, Phys. Rev. C 80, 041304(R) (2009).</p> <p>[8] J. T. Matta, U. Garg, W. Li, S. Frauendorf, A. D. Ayangeakaa, D. Patel, K. W. Schlabach, R. Palit, S. Saha,</p> |
|---|--|

- J. Sethi, *et al.*, Phys. Rev. Lett. **114**, 082501 (2015).
- [9] S. Frauendorf and F. Dönau, Phys. Rev. C **89**, 014322 (2014).
- [10] Q. B. Chen, S. Q. Zhang, P. W. Zhao, and J. Meng, Phys. Rev. C **90**, 044306 (2014).
- [11] Q. B. Chen, S. Q. Zhang, and J. Meng, Phys. Rev. C **94**, 054308 (2016).
- [12] Q. B. Chen, S. Q. Zhang, P. W. Zhao, R. V. Jolos, and J. Meng, Phys. Rev. C **94**, 044301 (2016).
- [13] K. Tanabe and K. Sugawara-Tanabe, Phys. Rev. C **95**, 064315 (2017).
- [14] A. A. Raduta, R. Poenaru, L. Gr. Ixaru, Phys. Rev. C **96**, 054320 (2017).
- [15] S. Frauendorf, Phys. Rev. C **97**, 069801 (2018).
- [16] K. Tanabe and K. Sugawara-Tanabe, Phys. Rev. C **97**, 069802 (2018).
- [17] M. Shimada, Y. Fujioka, S. Tagami, Y. R. Shimizu, Phys. Rev. C **97**, 024318 (2018).
- [18] R. Budaca, Phys. Rev. C **97**, 024302 (2018).
- [19] E. Streck, Q. B. Chen, N. Kaiser, and U.-G. Meißner, Phys. Rev. C **98**, 044314 (2018).
- [20] S. Biswas, R. Palit, S. Frauendorf, U. Garg, W. Li, G. H. Bhat, J. A. Sheikh, J. Sethi, S. Saha, Purnima Singh, *et al.*, arXiv: **nucl-ex**, 1608.07840
- [21] J. Simpson, Z. Phys. A **358** 139 (1997).
- [22] J. N. Scheurer, M. Aiche, M. M. Aléonard, G. Barreau, F. Bourguine, D. Boivin, D. Cabaussel, J. F. Chemin, T. P. Doan, J. P. Goudour *et al.*, Nucl. Instrum. Methods **A 385**, 501 (1997).
- [23] J. Gál, G. Hegyesi, J. Molnár, B. M. Nyakó, G. Kalinka, J. N. Scheurer, M. M. Aléonard, J. F. Chemin, J. L. Pedroza, K. Juhász *et al.*, Nucl. Instrum. Methods **A 516**, 502 (2004).
- [24] D. C. Radford, Nucl. Instrum. Meth. **A 361**, 297 (1995).
- [25] P. M. Jones, L. Wei, F.A. Beck, P. A. Butler, T. Byrski, G. Duchêne, G. de France, F. Hannachi, G. D. Jones, B. Kharraja, Nucl. Instrum. Methods **A 362**, 556 (1995).
- [26] G. Duchêne, F. A. Beck, P. J. Twin, G. de France, D. Curien, L. Han, C. W. Beausang, M. A. Bentley, P. J. Nolan, J. Simpson, Nucl. Instrum. Methods **A 432**, 90 (1999).
- [27] K. Starosta, T. Morek, Ch. Droste, S. G. Rohoziński, J. Srebrny, A. Wierzchucka, M. Bergström, B. Herskind, E. Melby, T. Czosnyka *et al.*, Nucl. Instrum. Methods **A 423**, 16 (1999).
- [28] K. S. Krane, R. M. Steffen, and R. M. Wheeler, Nucl. Data Tables **A 11**, 351 (1973).
- [29] F. A. Rickey, J. A. Grau, L. E. Samuelson, and P. C. Simms, Phys. Rev. C **15**, 1530 (1977).
- [30] B. Kruzsicz *et al.*, (to be published).
- [31] A. O. Macchiavelli, J. Burde, R. M. Diamond, C. W. Beausang, M. A. Deleplanque, R. J. McDonald, F. S. Stephens, and J. E. Draper, Phys. Rev. C **38**, 1088 (1988).
- [32] K. Nakai, Phys. Lett. **34B**, 269 (1971).
- [33] J. Meng, J. Peng, S. Q. Zhang, and S.-G. Zhou, Phys. Rev. C **73**, 037303 (2006).
- [34] J. Meng, ed., *Relativistic density functional for nuclear structure*, vol. 10 of *International Review of Nuclear Physics* (World Scientific, Singapore, 2016).
- [35] S. Frauendorf and J. Meng, Z. Phys. A **356**, 263 (1996).
- [36] S. Frauendorf and J. Meng, Nucl. Phys. **A617**, 131 (1997).
- [37] I. Hamamoto, Phys. Rev. C **65**, 044305 (2002).
- [38] W. X. Shi and Q. B. Chen, Chin. Phys. C **39**, 054105 (2015).
- [39] P. W. Zhao, Z. P. Li, J. M. Yao, and J. Meng, Phys. Rev. C **82**, 054319 (2010).
- [40] P. Ring and P. Schuck, *The nuclear many body problem* (Springer Verlag, Berlin, 1980).
- [41] C. S. Wu and J. Y. Zeng, High Energy Phys. Nucl. Phys. **9**, 214 (1985), (in Chinese).
- [42] C. S. Wu and J. Y. Zeng, Commun. Theor. Phys. **8**, 51 (1987).
- [43] Y. Y. Wang, Z. Shi, Q. B. Chen, S. Q. Zhang, and C. Y. Song, Phys. Rev. C **93**, 044309 (2016).
- [44] S. Frauendorf and F. Dönau, Phys. Rev. C **92**, 064306 (2015).